Chapter 18
Seismic Stability of Slopes Reinforced with Micropiles—A Numerical Study

Priyanka Ghosh[ID]**, Surya Kumar Pandey, and S. Rajesh**

18.1 Introduction

Slopes are either a naturally available soil profile which can be seen in most of the hilly regions or an engineered structure to serve various construction projects. Be it a natural or human-made structure, it needs to be analyzed carefully, which remains a challenging task in the field of geotechnical engineering. The failure of slopes under any condition may lead to tremendous loss to the society, which advocates for improving the soil to enhance the stability of slopes. Out of various ground improvement techniques, micropiles can be adopted to enhance the stability of such slopes. Micropiles are generally found to be versatile for serving various functions such as seismic retrofitting and underpinning (Elaziz and Naggar 2014; Elkasabgy and Naggar 2007; FHWA 2005; Kyung et al. 2017; Sun et al. 2013). Geotechnical engineers frequently use the stability charts proposed by Taylor (1937, 1948) to analyze a slope under the static condition. Various theoretical solutions were also recommended by different researchers (Bishop 1955; Chen 1975; Janbu 1954; Michalowski 1995, 2002; Spencer 1967) to determine the FOS of a slope under the static condition. However, these theories are mainly confined to static condition. To incorporate the effect of an earthquake, the theories mentioned above can be modified by including the seismic inertial forces. Therefore, an investigation on the static and the seismic stability of a slope reinforced with micropiles demands serious attention. Mononobe–Okabe theory (Mononobe and Matsuo 1929; Okabe 1926) marked the beginning of an evolution of the seismic analysis using the pseudo-static (PS) approach. After that, several researchers explored the seismic stability of a slope using the PS approach, which did not consider the effect of shear (V_s) and primary (V_p) wave velocities in the analysis and generated conservative results. In order to overcome the constraints posed by the PS approach, the original

P. Ghosh (✉) · S. K. Pandey · S. Rajesh
Department of Civil Engineering, IIT Kanpur, Kanpur 208016, India
e-mail: priyog@iitk.ac.in

pseudo-dynamic (OPD) approach (Choudhury and Nimbalkar 2005; Ghosh 2008; Ghosh and Kolathayar 2011; Nimbalkar et al. 2006; Steedman and Zeng 1990) is considered in the present study. The seismic stability of a slope reinforced with micropiles is evaluated using the limit equilibrium method (LEM) considering c-ϕ soil. The study is performed by assuming a circular slip surface passing through the toe of the slope. The effect of different parameters such as horizontal (k_h) and vertical (k_v) seismic acceleration coefficients, slope angle (i), angle of internal friction of the soil (ϕ), amplification factor (f_a) and angle of inclination of micropile (θ_b) on the stability of a slope is explored in terms of FOS. Under the seismic condition, the stability of a slope with micropiles is found to be affected less compared to that of a slope without micropiles.

18.2 Problem Definition

The stability of a slope is expected to get improved with the use of micropiles. However, the study on the effect of seismicity on the stability of micropile-reinforced slope is limited. In this study, a finite slope of height (H) and inclination (i) reinforced with vertical as well as inclined micropiles is considered under the static and the seismic conditions (Fig. 18.1). The mechanical properties of the soil include the internal friction angle (ϕ), cohesion (c) and unit weight (γ). The limit equilibrium method, coupled with the OPD approach, is adopted in the analysis. The slip surface is reasonably assumed to be circular (Fellenius 1936), which passes through the toe of the slope. The main objective is to determine the factor of safety of the slope reinforced with micropiles under both static and seismic conditions.
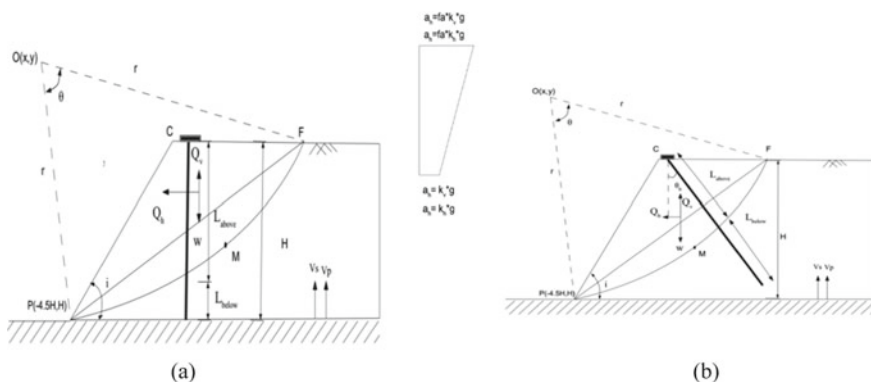

Fig. 18.1 Failure mechanism and associated forces with **a** vertical micropile and **b** inclined micropile

18.3   Assumptions

The following assumptions are made in the present study.

- The shear modulus of the soil is assumed to be constant throughout the height of the slope.
- The length of micropiles is considered to be uniform and always intersects the slip surface.
- The resistance of the pile cap is not considered in the analysis, and the micropile is assumed to be a fixed head pile.
- Location of the micropile is assumed at the top of the slope.
- Allowable displacement at the ground line is assumed 10% of the pile diameter (d) for the computation of the lateral capacity (Kyung and Lee 2018).
- The micropile is assumed to be a type-A-driven pile.

18.4   Methodology

18.4.1   Seismic Accelerations

In any earthquake event, the soil mass is subjected to seismic inertial forces developed due to the seismic accelerations. The easiest way to consider the seismic accelerations in the soil mass is the inclusion of uniform seismic acceleration coefficients throughout the soil body, as recommended by the PS approach. However, in reality, the seismic waves generated from any seismic event need not be in the same phase throughout the soil body. Moreover, these waves generally get amplified near the free surface. The phase change and amplifying nature of the seismic waves can be captured by the OPD approach, as proposed by Steedman and Zeng (1990). The OPD approach was also supported by a series of centrifuge experiments (Zeng and Steedman 1993). Considering these issues, the present investigation is performed using the OPD approach.

In the presence of a seismic excitation applied at the base of a slope, the soil mass at any depth (z) below the top surface and time (t) receives the horizontal (a_h) and the vertical (a_v) seismic accelerations, which can be expressed as

$$a_h(z,t) = \left[1 + \frac{H-z}{H}(f_a - 1)\right] k_h g \sin\left[\omega\left(t - \frac{H-z}{V_s}\right)\right] \tag{18.1}$$

$$a_v(z,t) = \left[1 + \frac{H-z}{H}(f_a - 1)\right] k_v g \sin\left[\omega\left(t - \frac{H-z}{V_p}\right)\right] \tag{18.2}$$

where H, f_a, V_s and V_p are the height of the slope, amplification factor, shear and primary wave velocity, respectively.

18.4.2 Stability Analysis with Vertical Micropiles

The stability of the slope is analyzed using the Fellenius method (Fellenius 1936), where the critical slip surface is obtained based on the minimum magnitude of the FOS. The mode of failure is considered as the toe failure, and hence, the circular slip surface always passes through the toe of the slope, as shown in Fig. 18.1a. The micropile of length L is placed vertically in such a way that it always intersects the slip surface. The horizontal (Q_h) and vertical (Q_v) seismic inertia forces are computed using the OPD approach as discussed earlier. The direction of Q_h and Q_v, as shown in Fig. 18.1a, is considered based on the recommendation in the literature. The forces acting on a micropile can be divided into two parts: axial and lateral forces. The axial force acting on a micropile is assumed to be equal to the axial capacity of the micropile at the limiting condition. The axial capacity of a micropile (P_{axi}) is generally governed by the geotechnical bond capacity and the structural capacity requirement. The allowable compressive load capacity of a micropile (P_G) based on the geotechnical bond requirement can be expressed as

$$P_G = \frac{\alpha_{bond}\pi d L_{above}}{SF} \tag{18.3}$$

where α_{bond} is the bond capacity between the pile and the soil, which depends on the type of pile; L_{above} is the length of the micropile above the slip surface, as shown in Fig. 18.1; and SF is the safety factor and generally taken as 2 as per FHWA (2005).

On the contrary, according to FHWA (2005), the allowable compressive load capacity of a type-A micropile (P_C) based on the structural requirement can be expressed as

$$P_C = 0.4 f_c A_{grout} + 0.47 f_y A_{casing} \tag{18.4}$$

where A_{grout} and A_{casing} are the cross-sectional area of the grout and the casing, respectively; and f_c and f_y are the compressive strength of the grout and the yield strength of the casing, respectively.

The axial capacity of a micropile (P_{axi}) is considered as the minimum of the capacity obtained from Eqs. 18.3 and 18.4. Similarly, the lateral capacity of a micropile (P_{lat}) can be determined based on the strength and the serviceability criteria (Murthy and Subba Rao 1995). Hence, by considering the equilibrium of forces, the FOS can be expressed as

$$FOS = \frac{(C_m + R\sin\phi)r + P_{lat}l_v + P_{axi}l_h}{Q_h\bar{y} + (W - Q_v)\bar{x}} \tag{18.5}$$

where C_m is the shear resistance mobilized along the slip surface, R is the reaction force exerted by the soil, r is the radius of the circular slip surface, $\bar{x}$ and $\bar{y}$ are the coordinates of the center of gravity of the failure wedge CFP with respect to the center of rotation O (Fig. 18.1), W is the self-weight of the failure wedge CFP, and l_v and l_h are the lever arms for the forces F_1 and F_2 respectively, where $F_1 = (P_{\text{lat}} - Q_h)$ and $F_2 = (P_{\text{axi}} + Q_v - W)$.

18.4.3   *Stability Analysis with Inclined Micropiles*

In case of an inclined micropile, the pile of length L is placed at a batter angle of θ_b with the vertical and passes through the circular slip surface as shown in Fig. 18.1b. Similar to a vertical micropile, the forces acting on an inclined micropile can be divided into two parts: axial and lateral forces. However, since the micropile is installed at a batter angle of θ_b, the axial force acts at an angle of θ_b with the vertical, whereas the lateral force is inclined at an angle, θ_b, with the horizontal. The axial capacity of an inclined micropile (P_{axi}) can be determined by following a similar procedure as mentioned for a vertical micropile. However, it is found to be challenging to predict the lateral capacity of an inclined micropile as the mobilization mechanism of the lateral resistance changes when the batter angle varies (Murthy and Subba Rao 1995; Reese and Welch 1975). Murthy and Subba Rao (Murthy and Subba Rao 1995) proposed a simplified approach to compute the lateral capacity of an inclined micropile (P_{lat}), where P_{lat} can be expressed based on the lateral capacity of a vertical micropile and the variation of the soil modulus. After determining the magnitude of P_{axi} and P_{lat} of an inclined micropile, the FOS for the slope can be determined from Eq. 18.5 just by replacing the respective parameters applicable to an inclined micropile.

18.5   **Results and Discussion**

Following the procedure, as discussed earlier, the numerical computations are performed by writing computer code in MATLAB. To obtain the minimum FOS, the value of t/T in the OPD approach and the location of the center of rotation (O) are varied, where T is the period of lateral shaking. The range of input parameters used in this study is given in Table 18.1.

The magnitudes of H/λ and H/η are chosen in such a way that $V_p/V_s = 1.87$, which is valid for most of the geological materials (Das 1993), where $\lambda = TV_s$ and $\eta = TV_p$. It is worth mentioning that H/λ and H/η represent the ratio of the time taken by the shear and the primary wave to travel the full height of the slope, respectively, to the period of lateral shaking (T).

The variation of FOS with k_h for a slope with vertical micropiles is presented in Fig. 18.2 for different values of ϕ. It can be seen that the FOS decreases

Table 18.1 Range of input parameters

Parameter	Range
ϕ	25–45°
f_a	1–1.6
k_h	0–0.2
k_v	0–k_h
i	30–45°
d	0.23–0.27 m
L/H	0.5–1
θ_b	−30–30°
c	5 kPa
γ	20 kN/m^3
f_c	27.6 MPa
f_y	552 MPa
α_{bond}	140 kPa

significantly with an increase in the magnitude of k_h and k_v. The recommended minimum static and seismic factors of safety for the micropiled structure as per FHWA (2005) are also presented in Fig. 18.2 just to show the limiting condition. The slope and the micropile parameters used in the analysis are given in Table 18.1.

The variation of FOS with L/H ratio for a slope with micropiles is shown in Fig. 18.3 for different values of ϕ and θ_b. It can be observed that the FOS increases with an increase in the magnitude of L/H ratio. This may be attributed to the fact that with an increase in the length of micropile, the length of micropile beyond the slip surface increases which offers higher pullout resistance due to the interaction between the grout and the soil. It can be also seen from Fig. 18.3b that the magnitude of FOS decreases with an increase in θ_b.

The variation of FOS with k_h for different values of H/λ and H/η is presented in Fig. 18.4. It can be observed that the FOS increases with an increase in the
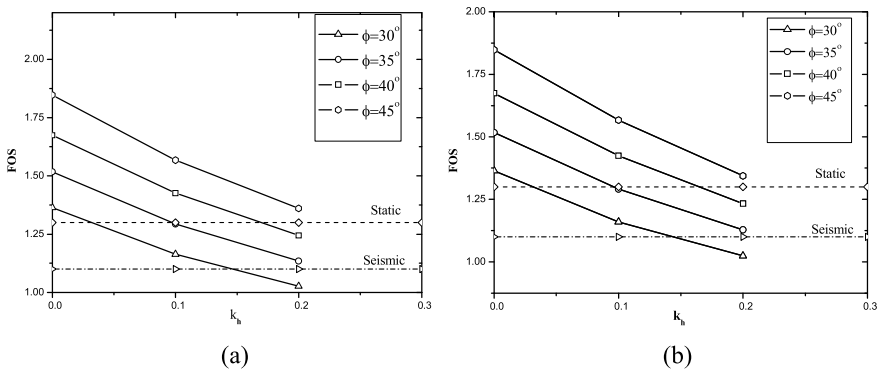

Fig. 18.2 Variation of FOS with k_h for different values of ϕ with $i = 30°$, $d = 0.23$ m, $f_a = 1$, $H/\lambda = 0.3$, $H/\eta = 0.16$ and $L/H = 1$. **a** $k_v = 0.5k_h$ and **b** $k_v = k_h$
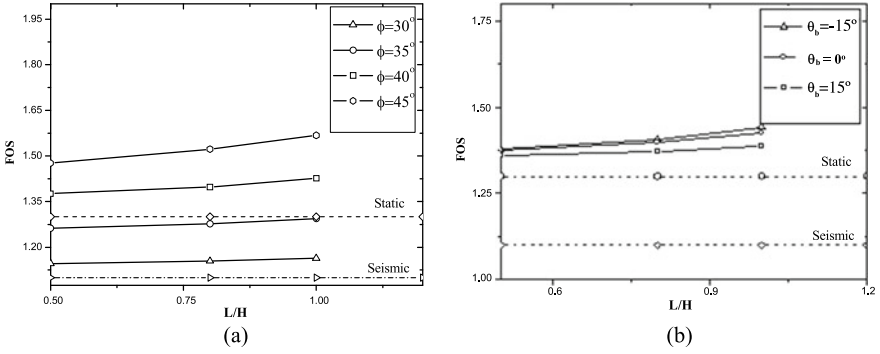
Fig. 18.3 Variation of FOS with *L/H* for **a** $\theta_b = 0°$ and **b** $\phi = 40°$ with $i = 30°$, $d = 0.23$ m, $f_a = 1$, $H/\lambda = 0.3$, $H/\eta = 0.16$, $k_h = 0.1$ and $k_v = 0.5k_h$

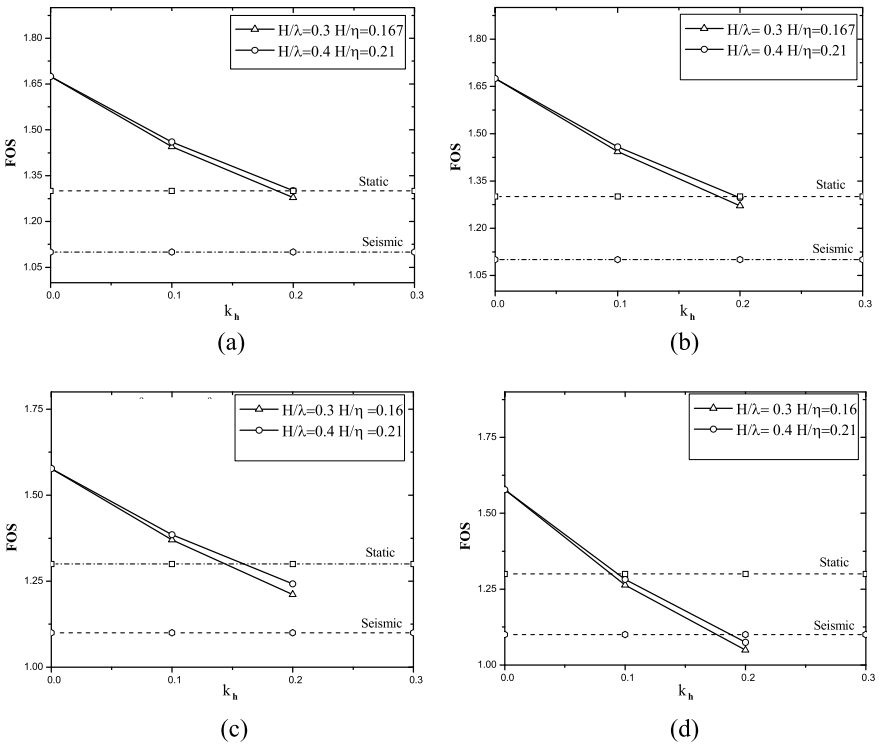**Fig. 18.4** Variation of FOS with k_h for different values of H/λ and H/η with $\phi = 40°$, $i = 30°$, $d = 0.23$ m, $f_a = 1$ and $L/H = 1$. **a** $\theta_b = 0$, $k_v = 0$, **b** $\theta_b = 0$, $k_v = 0.5k_h$, **c** $\theta_b = 15°$, $k_v = 0$, and **d** $\theta_b = 15°$, $k_v = 0.5k_h$

magnitude of H/λ and H/η. This may be attributed to the fact that with increase in H/λ and H/η, the velocity of shear and primary waves decreases, and thus, it reduces the effect of an earthquake.

The variation of FOS with k_h is shown in Fig. 18.5 for different values of i. It can be noted that the FOS decreases considerably with an increase in the magnitude of slope angle. This may be attributed to the fact that with an increase in i, the stability of a slope decreases which results in the reduction in FOS.

The variation of FOS with k_h is presented in Fig. 18.6 for different values of amplification factor (f_a). It can be seen that the FOS decreases with an increase in the magnitude of f_a. It may be attributed to the fact that with an increase in the amplification factor, the amplitude of acceleration increases, which in turn increases the seismic forces and, hence, the value of FOS decreases.

The variation of FOS with batter angle (θ_b) is presented in Fig. 18.7 for different values of ϕ under both static and seismic conditions. It is worth noting that positive
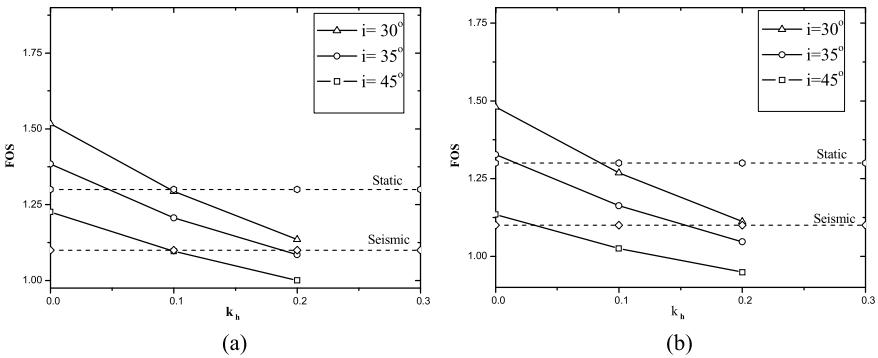

Fig. 18.5 Variation of FOS with k_h for different values of i with $\phi = 35°$, $d = 0.23$ m, $f_a = 1$, $H/\lambda = 0.3$, $H/\eta = 0.16$, $L/H = 1$ and $k_v = 0.5k_h$. **a** $\theta_b = 0$ and **b** $\theta_b = 15°$
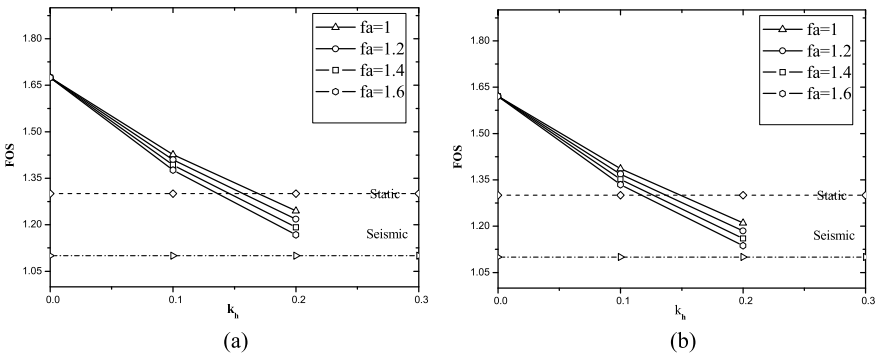

Fig. 18.6 Variation of FOS with k_h for different values of f_a with $\phi = 40°$, $i = 30°$, $d = 0.23$ m, $H/\lambda = 0.3$, $H/\eta = 0.16$, $L/H = 1$ and $k_v = 0.5k_h$. **a** $\theta_b = 0$ and **b** $\theta_b = 15°$

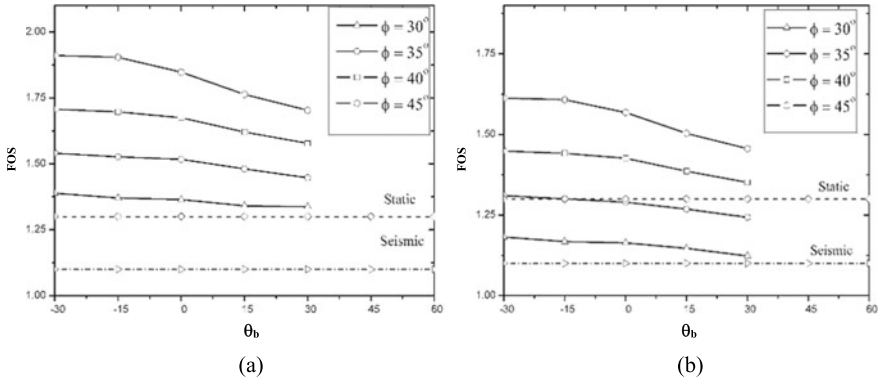**Fig. 18.7** Variation of FOS with θ_b for different values of ϕ with $i = 30°$, $d = 0.23$ m, $f_a = 1$, $H/\lambda = 0.3$, $H/\eta = 0.16$, $L/H = 1$ and $k_v = 0.5k_h$. **a** $k_h = 0$ and **b** $k_h = 0.1$

θ_b implies the angle between the axis of the micropile and the vertical direction in anticlockwise direction, whereas negative θ_b implies the angle in clockwise direction. It can be observed from Fig. 18.7 that the FOS decreases with an increase in the magnitude of θ_b. However, the reduction in the value of FOS is not found to be significant up to $\theta_b = -15°$. It may be attributed to the fact that the mobilized length (effective length) of the micropile above the slip surface decreases with an increase in the batter angle and, thus, there exists a reduction in the axial resistance.

In Fig. 18.8, the variation of FOS with k_h is presented for different values of micropile diameter (d). It can be observed from Fig. 18.8 that the FOS increases with an increase in the magnitude of d. This may be attributed to the fact that the axial and the lateral resistances of a micropile increase with an increase in the diameter of micropile.

Fig. 18.8 Variation of FOS with k_h for different values of d with $i = 30°$, $\phi = 35°$, $\theta_b = 15°$, $f_a = 1$, $H/\lambda = 0.3$, $H/\eta = 0.16$, $L/H = 1$ and $k_v = 0.5k_h$
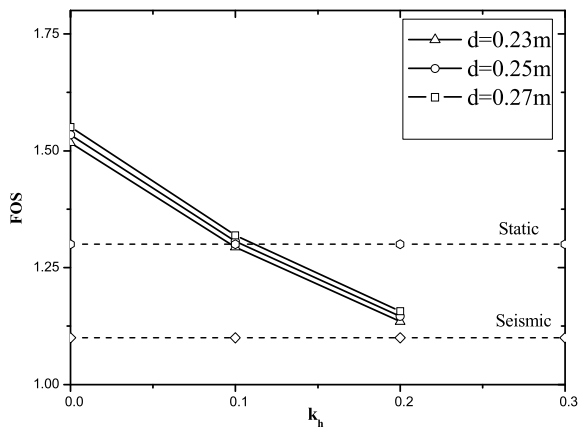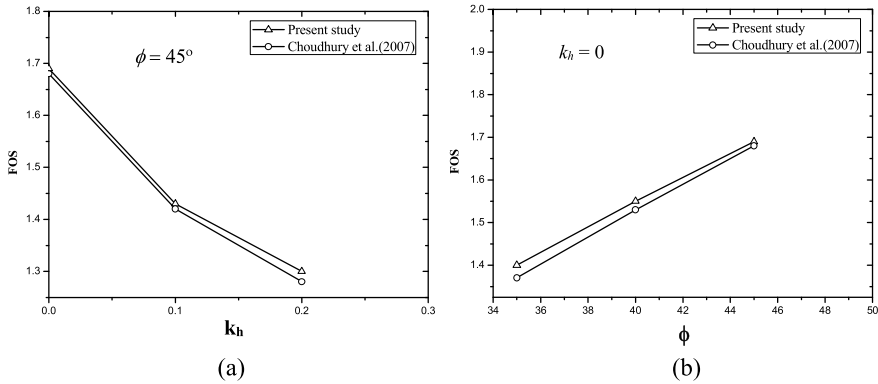
Fig. 18.9 Comparison of FOS for different values of **a** k_h and **b** ϕ with $i = 30°$, $d = 0.23$ m, $H = 10$ m, $c = 5$ kPa, $f_a = 1$, $H/\lambda = 0.3$, $H/\eta = 0.16$, $L/H = 1$ and $k_v = 0.5k_h$

18.6 Comparison

Studies on the seismic stability of a slope reinforced with micropiles are limited in the literature. Majority of the investigations available in the literature address the seismic slope stability analysis using the pseudo-static approach, which are unable to capture the time history and the phase effect of seismic accelerations. However, the present slope stability analysis was carried out by assuming a circular slip surface along with the original pseudo-dynamic approach in the presence of micropiles. Hence, an effort is made to obtain the seismic stability of a conventional slope without micropiles using the original pseudo-dynamic approach and compare the results with that obtained from the pseudo-static analysis available in the literature. In Fig. 18.9, the present results obtained for a slope without micropiles are compared with that reported by Choudhury et al. (2007) for different values of k_h and ϕ. It can be noticed that the present results compare reasonably well with that reported by Choudhury et al. (2007).

18.7 Conclusions

The following conclusions can be made from the results obtained from the present analysis.

- The FOS for a slope reinforced with micropiles decreases with an increase in the magnitude of k_h and k_v. Under both static and seismic conditions, the magnitude of FOS is found to increase by about 11% with an increase in ϕ from 30 to 45° at an interval of 5°.

- The FOS for a slope reinforced with micropiles increases with an increase in the length of micropiles. The magnitude of FOS is found to increase by 25% when the *L/H* ratio increases roughly by 25%. The enhancement in the FOS becomes more pronounced at a higher value of ϕ.
- The magnitude of FOS decreases with an increase in f_a but increases with an increase in *H/λ* and *H/η*.
- Under both static and seismic conditions, an increase in the diameter of micropiles from 0.23 to 0.27 m results around 3% higher FOS.
- Under the seismic condition, inclined micropiles are found to be more effective than vertical micropiles. The FOS generally decreases with an increase in the batter angle of micropiles.
- The FOS for a slope reinforced with micropiles is found to be conservative for the pseudo-static approach compared to the original pseudo-dynamic approach.

References

Bishop AW (1955) The use of the slip circle in the stability analysis of slopes. Geotechnique 5 (1):7–17

Chen WF (1975) Limit analysis and soil plasticity. Elsevier Science, Amsterdam, Netherlands

Choudhury D, Nimbalkar SS (2005) Seismic passive resistance by pseudo-dynamic method. Geotechnique 55(9):699–702

Choudhury D, Basu S, Bray JD (2007) Behaviour of slopes under static and seismic conditions by limit equilibrium method. In: Proceedings of Geo-Denver 2007: new peaks in geotechnics, Denver, Colorado, pp 1–10

Das BM (1993) Principles of soil dynamics. PWS-KENT, Boston, USA

Elaziz AYA, El Naggar MH (2014) Group behaviour of hollow-bar micropiles in cohesive soils. Can Geotech J 51(10):1139–1150

Elkasabgy MA, El Naggar MH (2007) Finite element analysis of the axial capacity of micropiles. 8th ISM Workshop, Toronto, ON, Canada

Fellenius W (1936) Calculation of stability of earth dams. In: Proceedings of 2nd Congress Large Dams, vol 4. Washington, USA, pp 445–462

FHWA (2005) Micropile design and construction. U.S. Department of Transportation, Federal Highway Administration, FHWA NHI-05-039

Ghosh P (2008) Seismic active earth pressure behind a non-vertical retaining wall using pseudo-dynamic analysis. Can Geotech J 45(1):117–123

Ghosh P, Kolathayar S (2011) Seismic passive earth pressure behind non vertical wall with composite failure mechanism: pseudo-dynamic approach. Geotech Geol Eng 29(3):363–373

Janbu N (1954) Application of composite slip surfaces for stability analysis. In: Proceedings of European conference on stability of earth slopes, Stockholm, Sweden, pp 43–49

Kyung D, Kim G, Kim D, Lee J (2017) Vertical load-carrying behavior and design models for micropiles considering foundation configuration conditions. Can Geotech J 54(2):234–247

Kyung D, Lee J (2018) Interpretative analysis of lateral load–carrying behavior and design model for inclined single and group micropiles. J Geotech Geoenviron Eng 144(1):04017105(1–11)

Michalowski RL (1995) Slope stability analysis: a kinematical approach. Geotechnique 45 (2):283–293

Michalowski RL (2002) Stability charts for uniform slopes. J Geotech Geoenviron Eng 128 (4):351–355

Mononobe N, Matsuo H (1929) On the determination of earth pressures during earthquake. In: Proceedings of world engineering conference, Tokyo, Japan, pp 177–185

Murthy VNS, Subba Rao KS (1995) Prediction of nonlinear behavior of laterally loaded long piles. In: Foundation Engineer, vol 1(2), New Delhi, India

Nimbalkar SS, Choudhury D, Mandal JN (2006) Seismic stability of reinforced-soil wall by pseudo-dynamic method. Geosynth Int 13(3):111–119

Okabe S (1926) General theory of earth pressures. J Jpn Soc Civil Eng 12(6):1277–1323

Reese LC, Welch RC (1975) Lateral loading of deep foundations in stiff clay. J Geotech Eng Div 101(7):633–649

Spencer E (1967) A method of analysis of the stability of embankments assuming parallel inter-slice forces. Geotechnique 17(1):11–26

Steedman RS, Zeng X (1990) The influence of phase on the calculation of pseudo-static earth pressure on a retaining wall. Geotechnique 40(1):103–112

Sun SW, Wang JC, Bian XL (2013) Design of micropiles to increase earth slopes stability. J Cent South Univ 20(5):1361–1367

Taylor DW (1937) Stability of earth slopes. J Boston Soc Civil Eng 24(3):197–246

Taylor DW (1948) Fundamentals of soil mechanics. Wiley, New York, USA

Zeng X, Steedman RS (1993) On the behaviour of quay walls in earthquakes. Geotechnique 43 (3):417–431